Supporting Information

Combination of large cation and coordinating additive improves carrier transport properties in quasi-2D perovskite solar cells

Sylvester Sahayaraj[1], Eros Radicchi[2,3], Marcin Ziółek[4], Mateusz Ścigaj[5], Magdalena Tamulewicz-Szwajkowska[6], Jarosław Serafińczuk[6], Filippo De Angelis[2,3,7], Konrad Wojciechowski[1,5]

[1]Saule Research Institute, Wroclaw Technology Park, 11 Dunska, 54-130 Wroclaw, Poland

[2]Department of Chemistry, Biology and Biotechnology, University of Perugia, via Elce di Sotto 8, 06123 Perugia, Italy

[3]Computational Laboratory for Hybrid/Organic Photovoltaics (CLHYO), CNR-ISTM, via Elce di Sotto 8, 06123 Perugia, Italy.

[4]Faculty of Physics, Adam Mickiewicz University, Uniwersytetu Poznańskiego 2, 61-614 Poznan, Poland.

[5]Saule Technologies, Wroclaw Technology Park, 11 Dunska, 54-130 Wroclaw, Poland.

[6]Department of Nanometrology, Faculty of Microsystem Electronics and Photonics, Wroclaw University of Science and Technology, Janiszewskiego 11/17, Wroclaw, Poland.

[7]CompuNet, Istituto Italiano di Tecnologia, Via Morego 30, 16163 Genova, Italy.

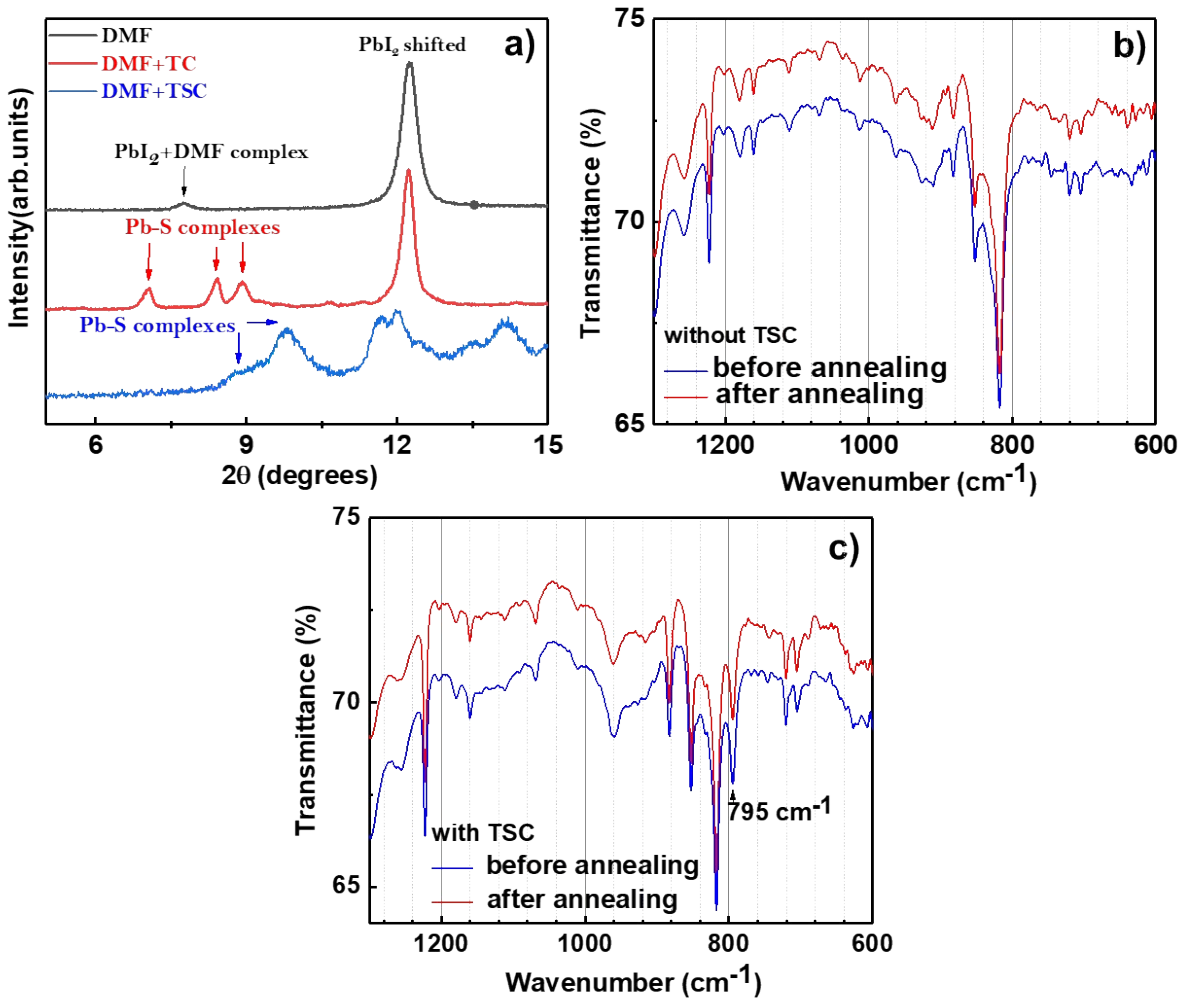

Figure S1. a) X-ray diffractograms (XRD) of PbI_2 films processed from the different DMF solutions; FTIR spectra of spin-coated perovskite films (before and after annealing), processed from the precursor solution a) without, and b) with the TSC additive.

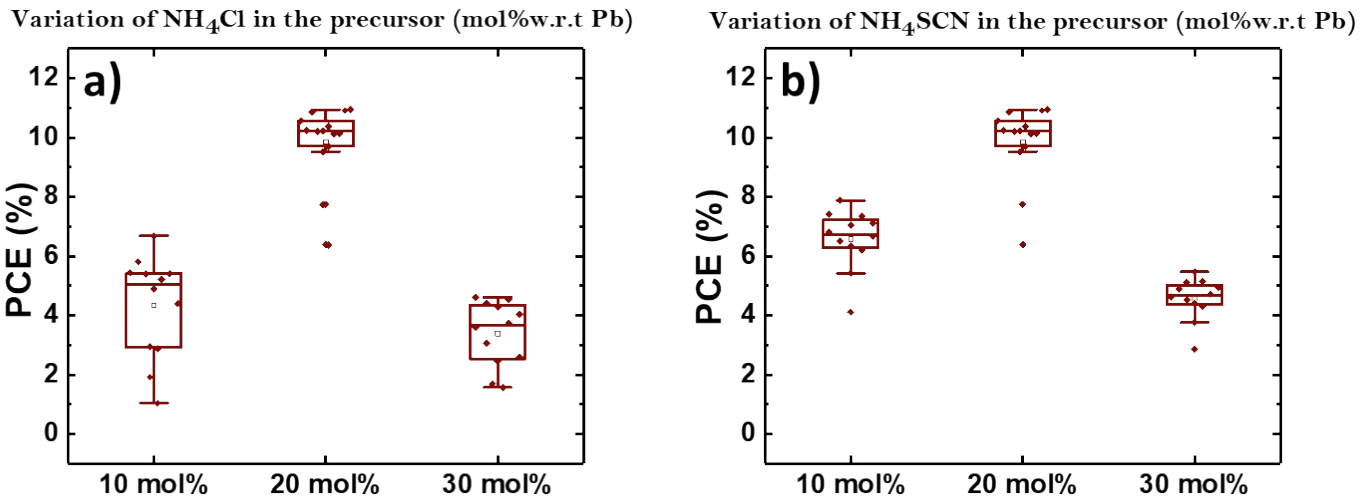

Figure S2. Graphical representation of the statistics of photovoltaic parameters extracted from the JV characterization measurements of a batch of quasi-2D perovskite solar cells, prepared with a) varied amount of NH_4Cl additive and fixed amount (20 mol%) of NH_4SCN, and b) varied amount of NH_4SCN additive and fixed amount (20 mol%) of NH_4Cl additive. Each dot corresponds to an individual solar cell.

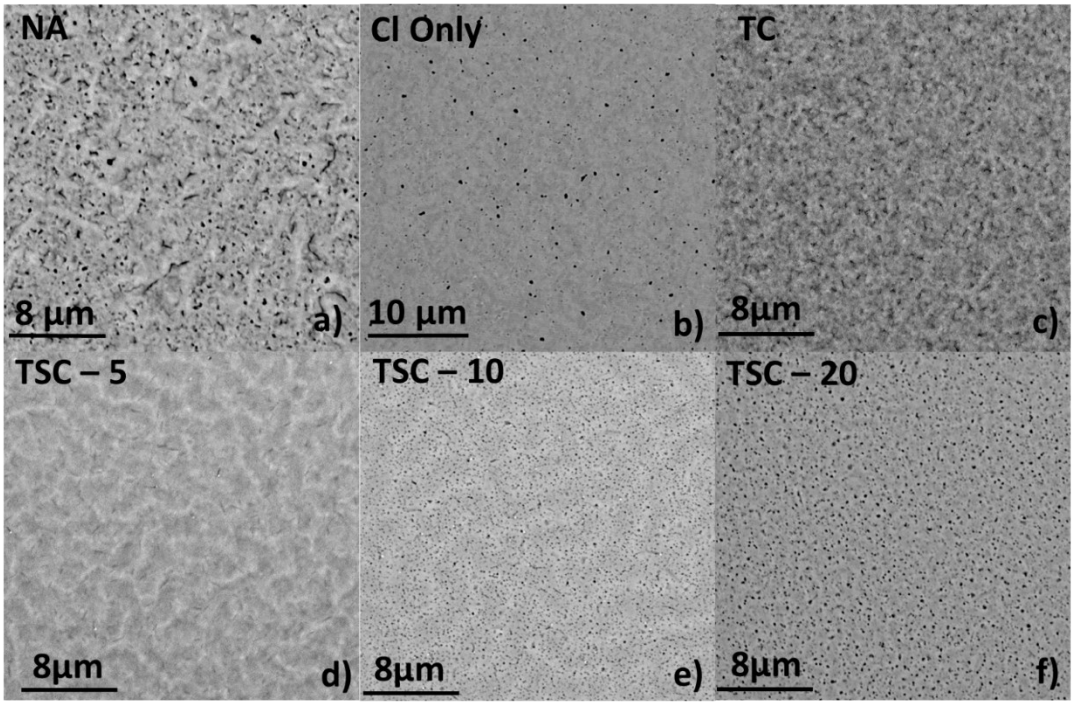

Figure S3. a- f) SEM images of quasi-2D perovskite films, with PEA^+ organic spacer, and different additive combinations.

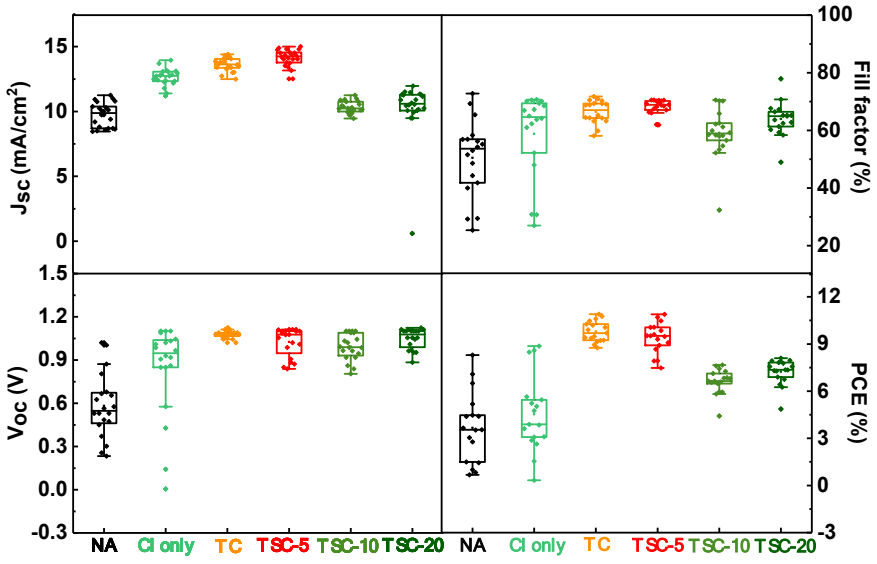

Figure S4. Graphical representation of the statistics of photovoltaic parameters extracted from the JV characterization measurements of a larger set of quasi-2D perovskite solar cells, prepared with PEA^+ organic spacer and different additive combinations. Each dot corresponds to an individual solar cell.

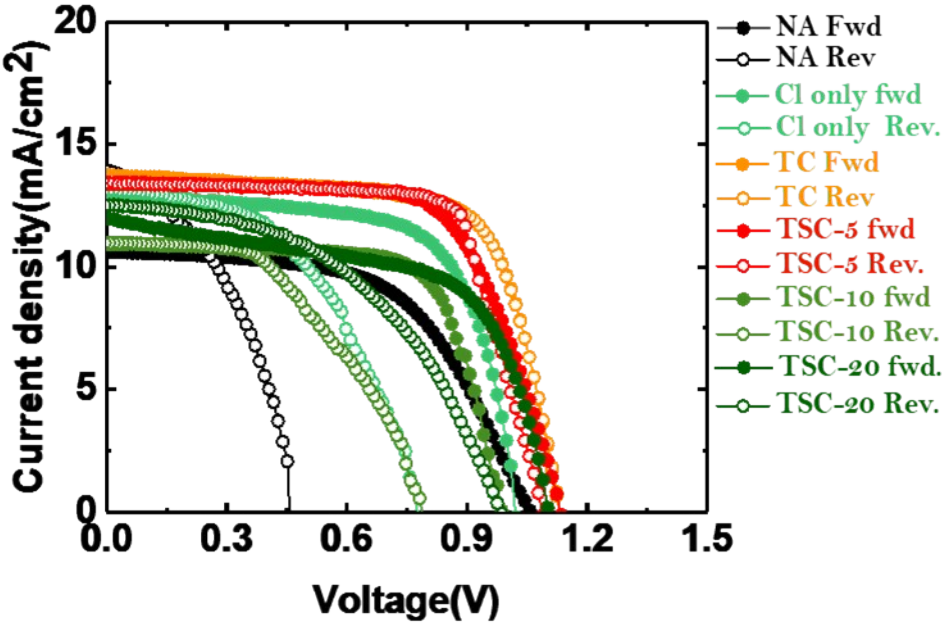

Figure S5. JV characteristics (forward and reverse scan directions) of quasi-2D perovskite solar cells, with PEA^+ organic spacer, and different additive combinations.

Table S1. Photovoltaic parameters extracted from the JV characterizations (shown in Figure S3) of quasi-2D perovskite solar cells, with PEA^+ organic spacer, and different additive combinations. The ratio of the SPO-derived and JV-derived efficiency is also provided.

Sample code	Scan direction	J_{sc} (mA/cm^2)	V_{oc} (V)	FF (%)	Efficiency (%)	PCE_{SPO} (%)	PCE_{SPO}/PCE_{IV}
No additives (NA)	Forward	10.8	1.02	59	8.3	-	-
	Reverse	14	0.45	38	2.8		
Cl^- only	Forward	13	1.08	62.12	8.9	7.9	0.88
	Reverse	13.3	0.78	49.7	5		
TC	Forward	13.6	1.12	71.6	10.9	11	1
	Reverse	13.8	1.12	70.6	11		
TSC-5	Forward	15	1.11	68	10.8	10.5	0.97
	Reverse	14.8	1.09	65	10.3		
TSC -10	Forward	12	0.92	75.8	7.7	7	0.91
	Reverse	11.05	0.52	52.9	3		
TSC – 20	Forward	11.4	1.1	62.5	7.9	7.3	0.92
	Reverse	12.1	0.96	49.2	5.8		

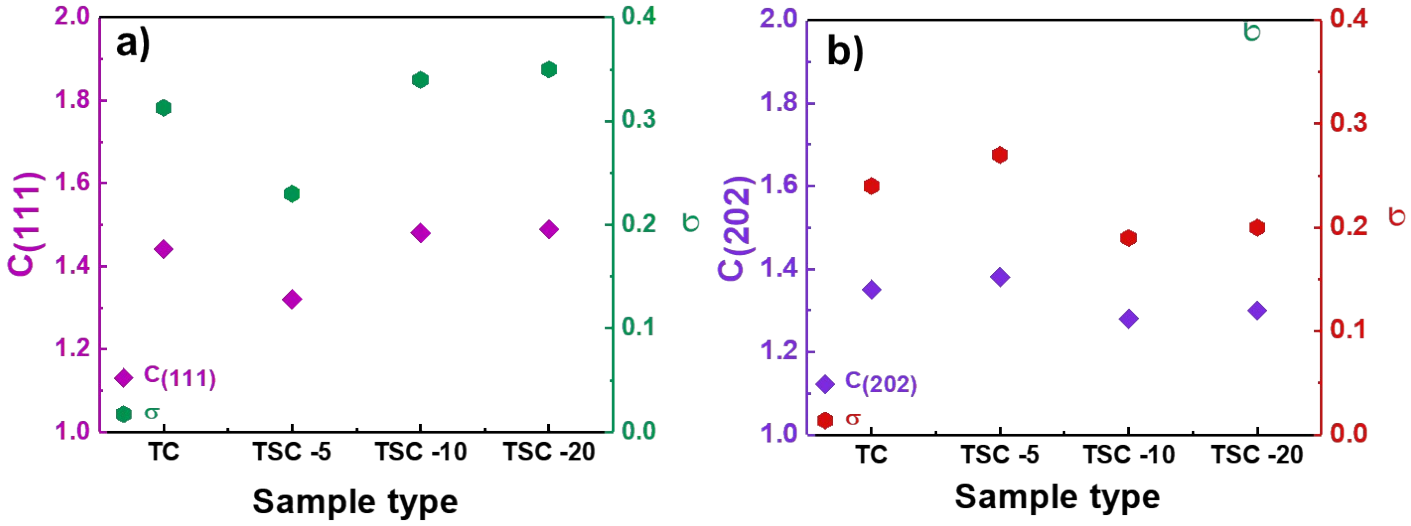

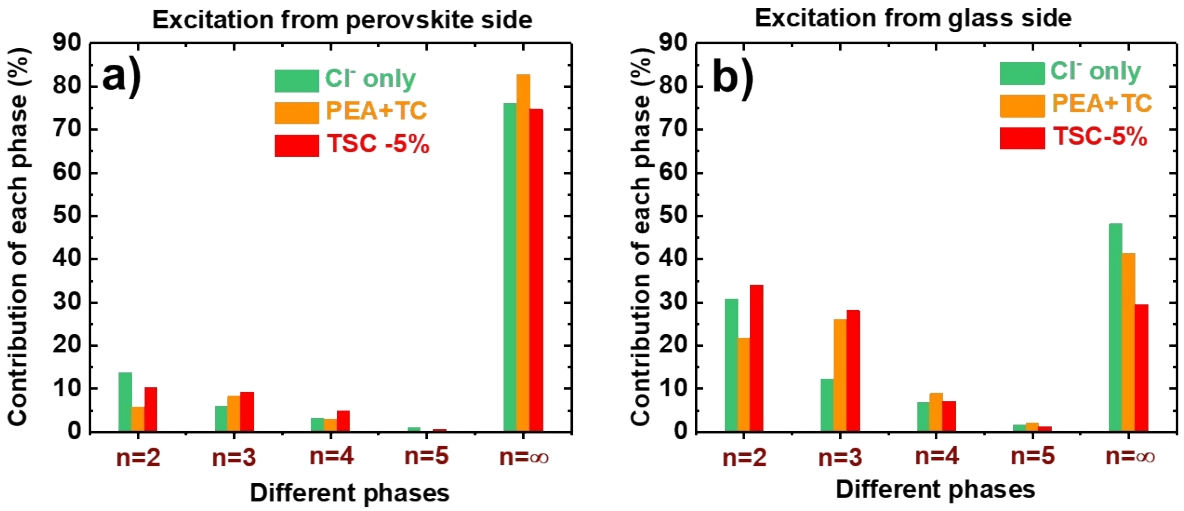

Figure S7. Representation of the proportion of different phases present in the quasi-2D perovskite films, when probed from the a) perovskite side, and b) glass side.

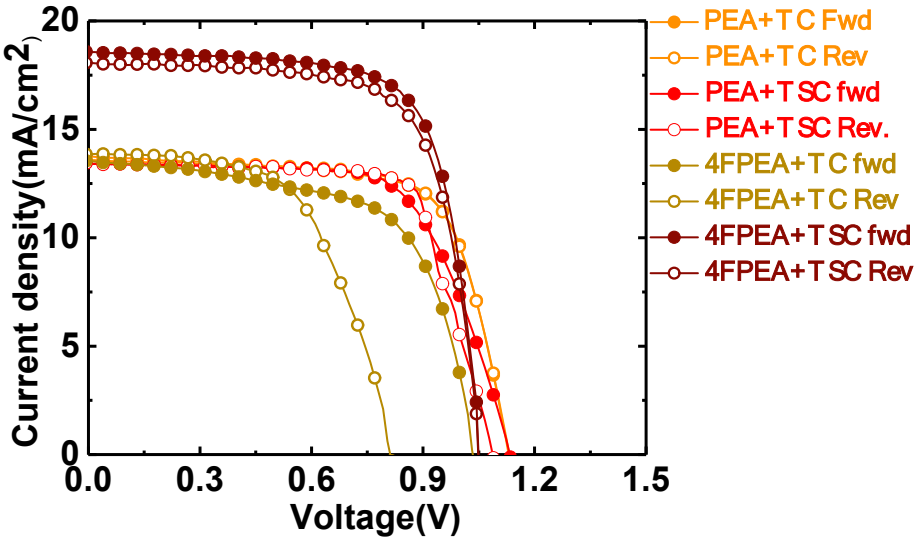

Figure S8. JV characteristics (forward and reverse scan directions) of quasi-2D perovskite solar cells, with different combinations of large cation and templating additive.

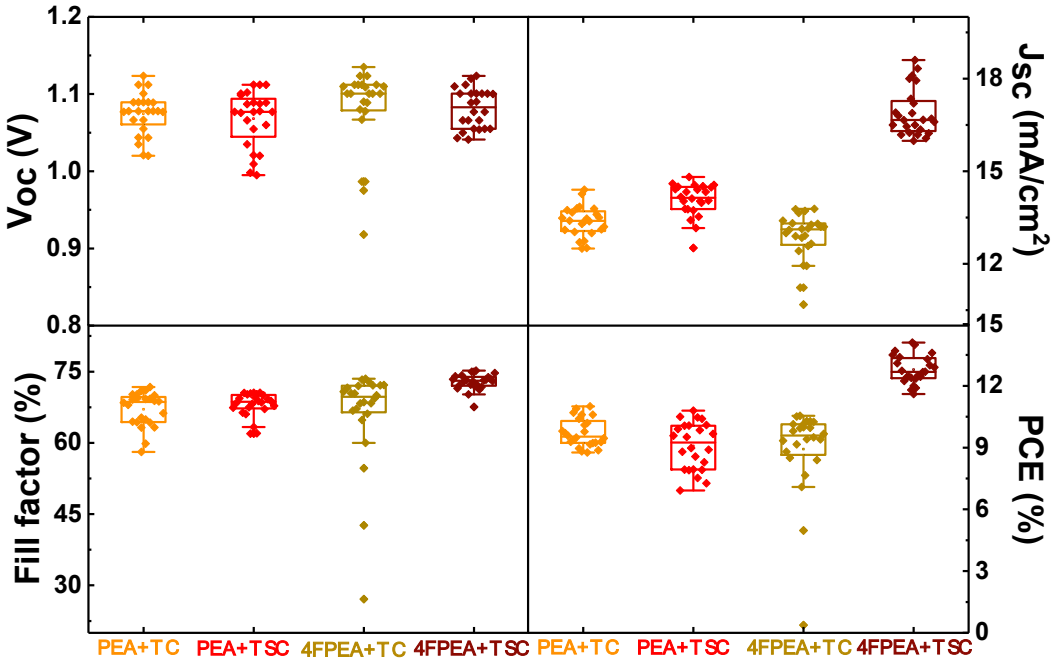

Figure S9. Graphical representation of the statistics of photovoltaic parameters extracted from the JV characterization measurements of a larger set of quasi-2D perovskite solar cells, prepared with different combinations of large cation and templating additive. Each dot corresponds to an individual solar cell.

Table S2. Photovoltaic parameters extracted from the JV characterizations (shown in Figure S7) of quasi-2D perovskite solar cells, prepared with different combinations of large cation and templating additive. The ratio of the SPO-derived and JV-derived efficiency is also provided.

Sample code	Scan direction	J_{sc} (mA/cm²)	V_{oc} (V)	FF (%)	Efficiency (%)	PCE_{SPO} (%)	PCE_{SPO}/PCE_{IV}
PEA + TC	Forward	13.6	1.12	71.6	10.9	11	1
	Reverse	13.8	1.12	70.6	11		
PEA + TSC	Forward	15	1.11	68	10.8	10.5	0.97
	Reverse	14.8	1.09	65	10.3		
4FPEA+TC	Forward	13.6	1.1	58.6	9.1	-	-
	Reverse	13.9	1.03	44.3	6.4		
4FPEA+TSC	Forward	18.6	1.05	73.2	14.06	13.8	0.98
	Reverse	18.1	1.05	71.5	13.6		

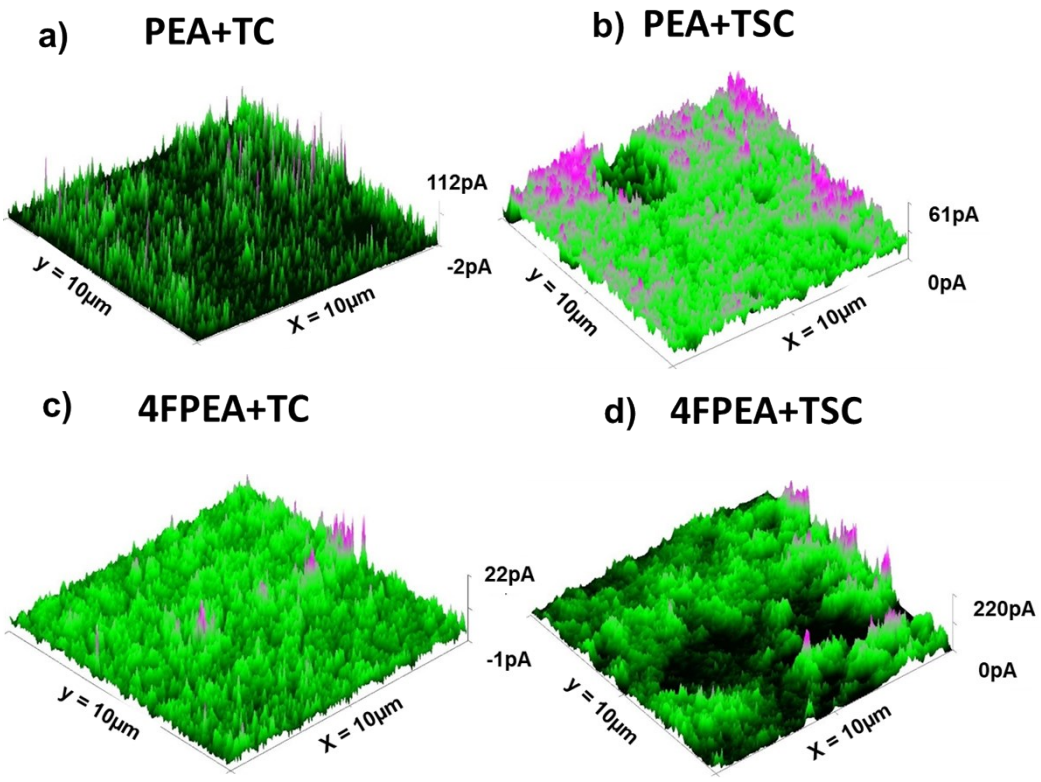

Figure S10. a- d) 3D current maps, obtained from c-AFM measurements, of different quasi-2D perovskite films, prepared with different combinations of large cation and templating additive.

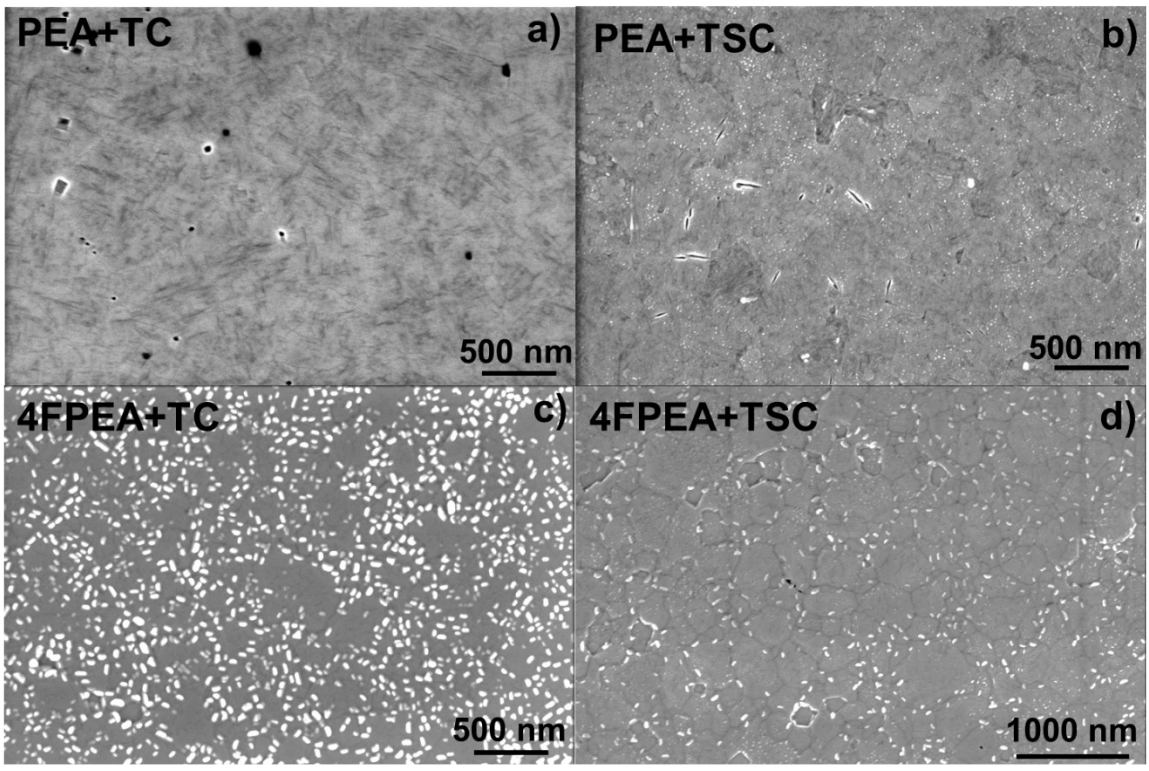

Figure S11. a-d) SEM images of quasi-2D perovskite films, prepared with different combinations of large cation and templating additive.

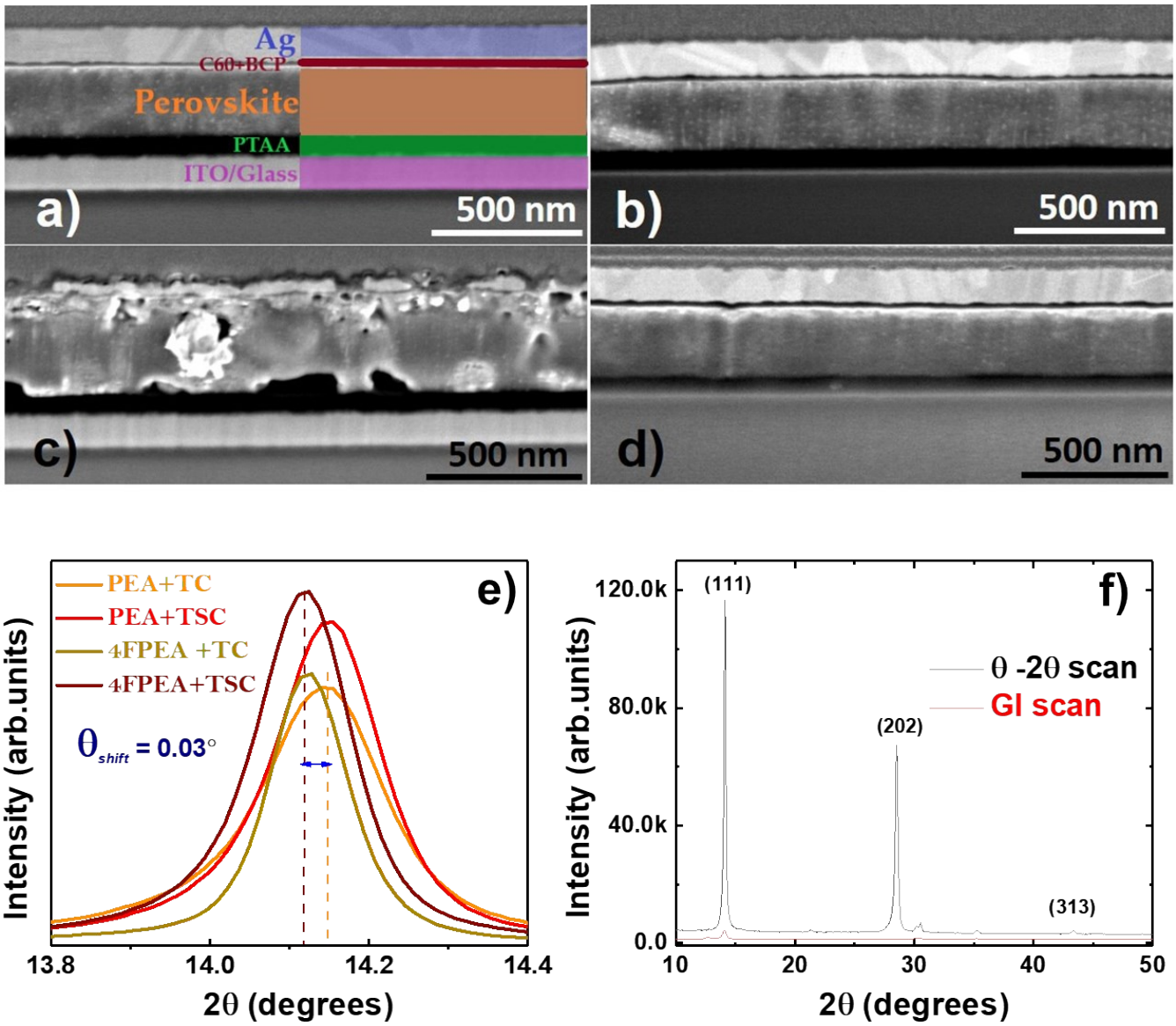

Figure S12. a-d) Cross-section SEM images of quasi-2D perovskite films, prepared with different combinations of large cation and templating additive; e) Zoomed-in section of the XRD pattern showing the change in the peak positions with the inclusion of 4F-PEAI; f) comparison of the conventional and grazing incidence XRD scan.

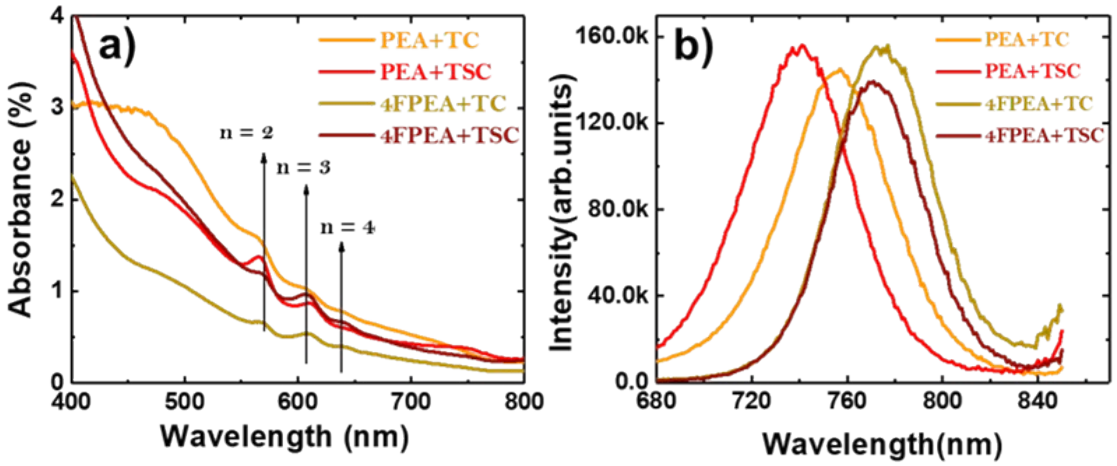

Figure S13. a) UV-Vis absorption spectra of quasi-2D perovskite films, prepared with different combinations of large cation and templating additive; b) steady-state photoluminescence spectra of the same samples.

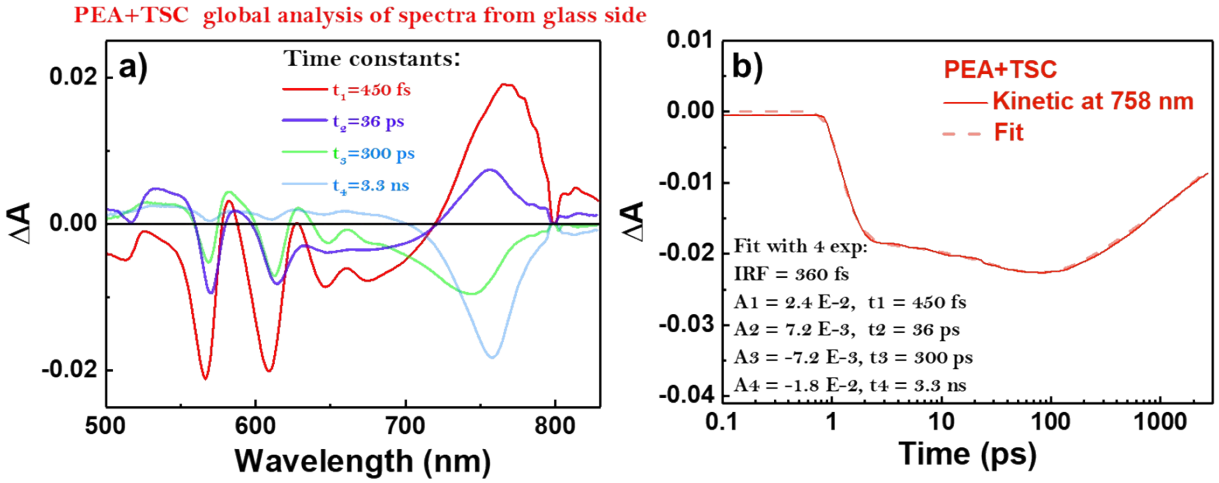

Figure S14. a) Global analysis of the decay of different phases, observed in the perovskite sample 'PEA+TSC', excited through the glass-side; b) 4-exponential fit for the bleach at 758 nm, with different time constant values, derived for the 'PEA+TSC' sample.

Transient absorption spectra were globally analysed with the Surface Explorer Software

Table S3. Proportion ratio for each phase identified in different quasi-2D perovskite films (different combinations of large cation and templating additive), counted as the phase contribution probed from the glass-side divided by its contribution probed from the perovskite-side.

Sample name	P_{glass}/P_{PVK} n =2	P_{glass}/P_{PVK} n =3	P_{glass}/P_{PVK} n=4	P_{glass}/P_{PVK} n=5	P_{glass}/P_{PVK} n =∞
PEA +TC	3.7	3.2	3.1	10	0.5
PEA +TSC	3.3	3.1	1.4	2.1	0.4
4FPEA +TC	2.7	3.1	2.5	1.8	0.5
4FPEA +TSC	**1**	**1.1**	**1**	**0.9**	**1**

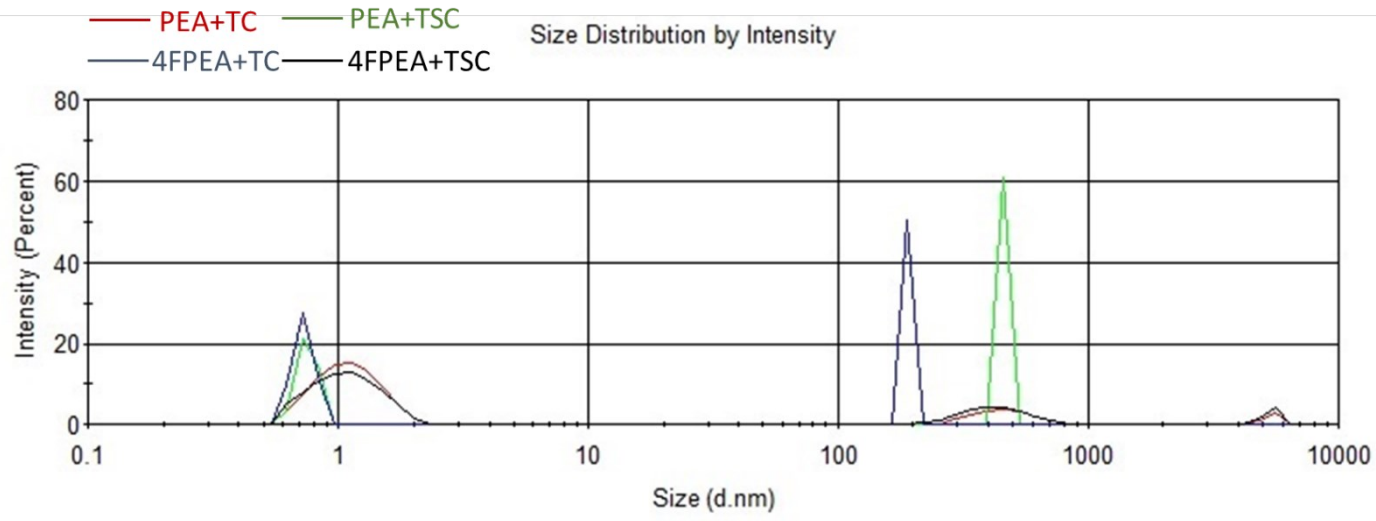

Table S4. Solubility of different organic iodides used for the formation of quasi-2D perovskite films in DMF.

Material	MAI	PEAI	4F-PEAI
Solubility (g/ml)	1.031	2.163	1.597
Solubility (mol/l)	5	4.5	4

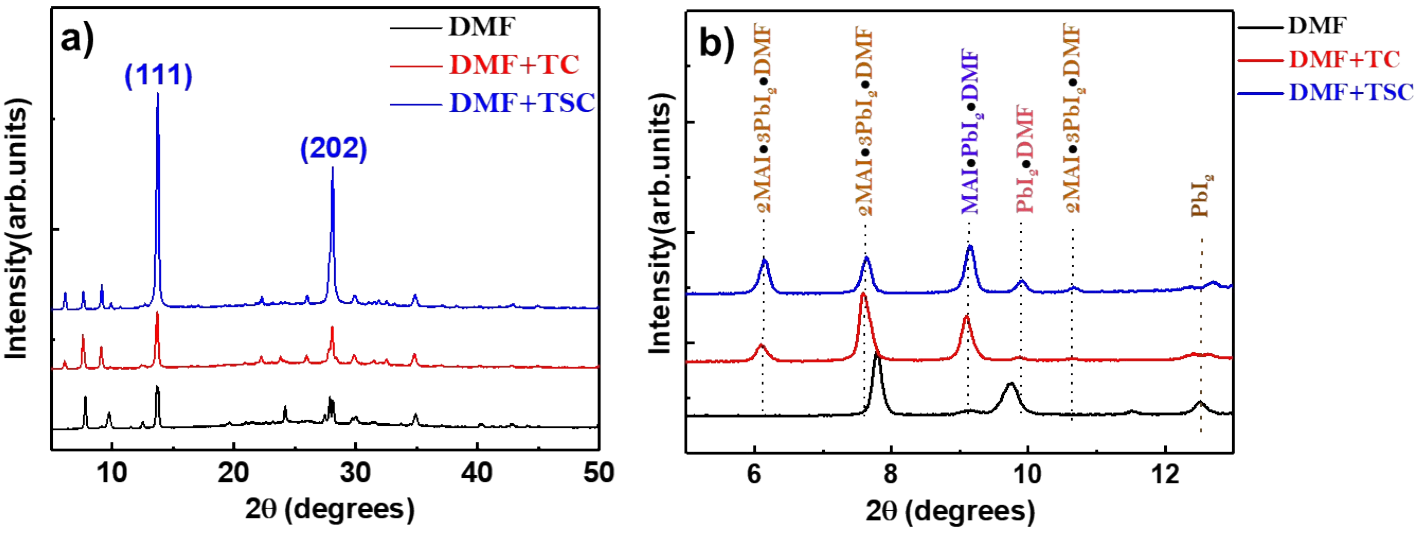

Figure S16. a) X-ray diffractograms (XRD) of MAI+PbI_2 films spin-coated from different DMF solutions; b) zoom-in at the low angle range depicting different intermediate phases.

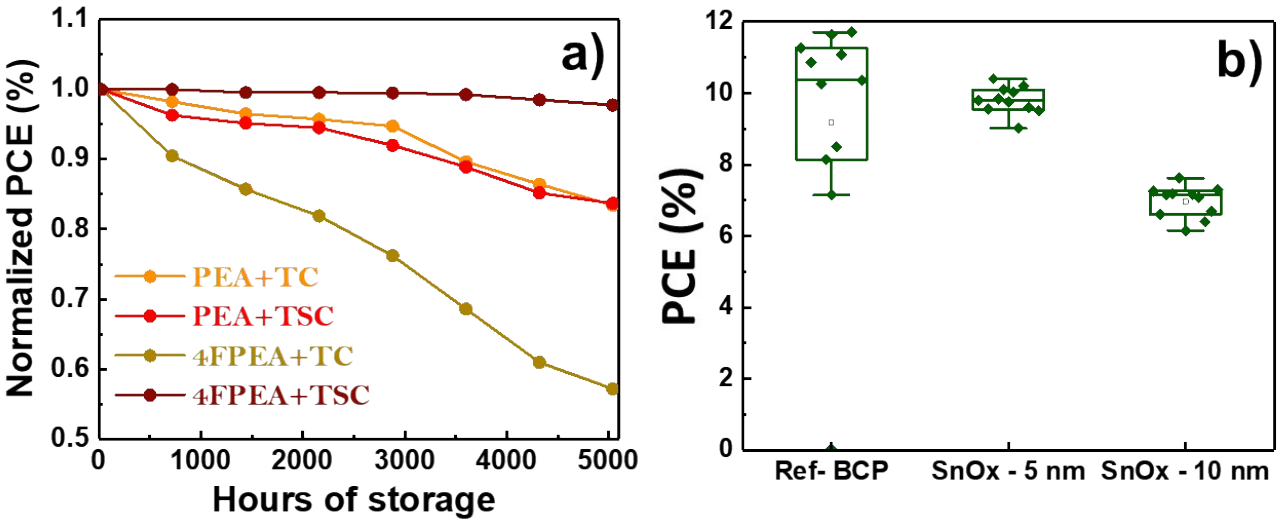

Figure S17. a) Normalized PCE evolution of quasi-2D perovskite solar cells (prepared with different combinations of large cation and templating additive) as a function of storage time in inert atmosphere; b) statistics of photovoltaic parameters extracted from the JV characterization measurements of quasi-2D perovskite solar cells, prepared with different buffer layers inserted before the back-contact electrode.